Fermi National Accelerator Laboratory

TM-1655

Longitudinal Emittance An Introduction to the Concept and Survey of Measurement Techniques Including Design of a Wall Current Monitor*

Robert C. Webber
Fermi National Accelerator Laboratory
P.O. Box 500
Batavia, Illinois 60510

March 1990

* To be published in the proceedings of the Workshop on Accelerator Instrumentation, Upton, New York, October 23-26, 1989.

LONGITUDINAL EMITTANCE

AN INTRODUCTION TO THE CONCEPT AND SURVEY OF MEASUREMENT TECHNIQUES INCLUDING DESIGN OF A WALL CURRENT MONITOR

Robert C. Webber
Fermi National Accelerator, Batavia, Il. 60510

ABSTRACT

The properties of charged particle beams associated with the distribution of the particles in energy and in time can be grouped together under the category of longitudinal emittance. This article is intended to provide an intuitive introduction to the concepts of longitudinal emittance; to provide an incomplete survey of methods used to measure this emittance and the related properties of bunch length and momentum spread; and to describe the detailed design of a 6 Ghz bandwidth resistive wall current monitor useful for measuring bunch shapes of moderate to high intensity beams. Overall, the article is intended to be broad in scope, in most cases deferring details to cited original papers.

INTRODUCTION TO LONGITUDINAL EMITTANCE

The focus of the present discussion is to be longitudinal properties of beams of accelerated particles. These properties include the energy, energy distribution, and time distribution of particles comprising a beam. Longitudinal emittance will be defined as a concept to quantify the distribution, in energy and time, of particles in a beam. Since accelerating fields are generally periodic, a phase variable often replaces the time variable.

Beams from even dc types of accelerators, such as ion sources, electron guns, Van de Graaffs, Cockcroft-Waltons, etc., usually display a time structure due to pulsed operation, random fluctuations in the beam current, or both. While these time structures are of interest to the designers and users of such beams, the dimension of time is not fundamental to the acceleration process. This clearly is not the case with accelerators utilizing periodically pulsed or rf fields to accelerate particles. There are only certain phases and amplitudes of the fields appropriate for stable particle acceleration. Time or phase becomes a fundamental parameter.

Consider Figure 1A. The positions of many particles, say from an ion source or electron gun, are plotted on a scale of energy and time. E_s has arbitrarily been defined to be the average energy of the distribution. Particles of the beam have some range of energies, but are distributed more or less uniformly in time. The energy spread implies a spread in velocities. The particles, therefore, move relative to each other. Arrows in the figure indicate this relative motion.

Now accelerate this beam with a sinusoidally varying field as in Figure 1B. Figure 1C results. The peak to peak energy spread has increased, but the time distribution is still uniform. Observed some time later, without additional acceleration, higher energy particles are seen to arrive early in time relative to lower energy companions as shown in Figure 1D. The beam has become bunched in time.

The motion of several particles can be followed through this process. Note that the phase coordinate has been chosen to move with the unaccelerated particle S, which therefore

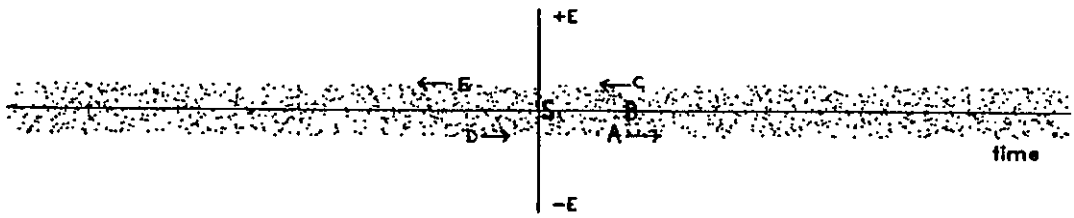

A. Coasting unbunched beam

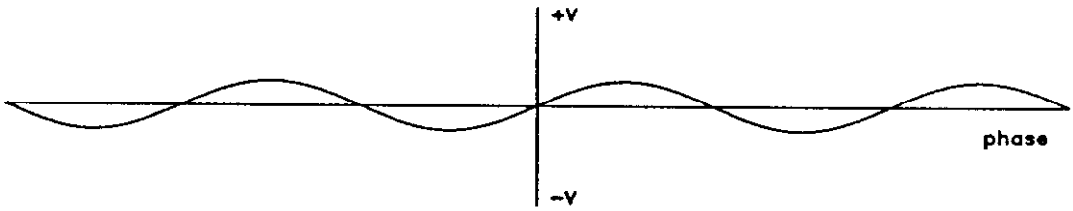

B. Accelerating voltage

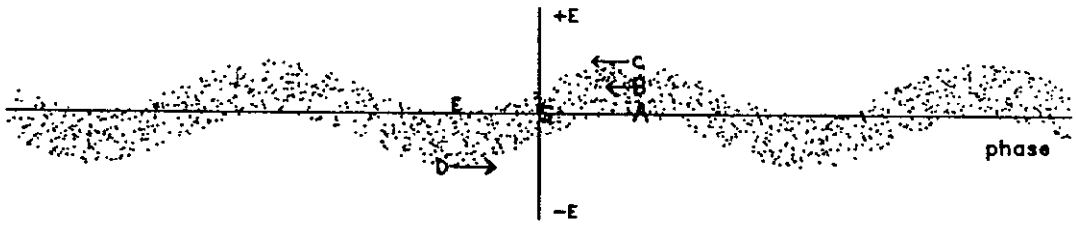

C. Beam immediately after acceleration

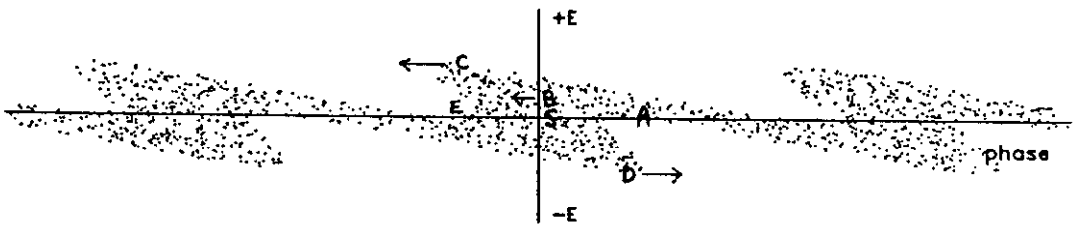

D. Beam bunched after drift

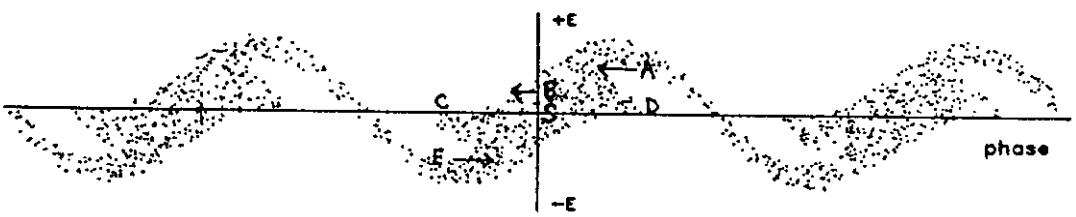

E. After second acceleration (at twice voltage)

FIGURE 1
BEAM DISTRIBUTIONS IN PHASE SPACE

remains fixed in both energy and phase. Particles **A**, **B**, and **C** are accelerated equal amounts. Particle **A** is accelerated to the same energy as particle S and then remains fixed in position. It undergoes motion on the energy coordinate, but not on the phase coordinate. **B** is accelerated to a higher energy than S and proceeds to travel earlier in time. **C** changes in energy the same amount as **A** and **B**, but, being the most energetic to begin with, moves most in phase relative to S. **E** and **D** are decelerated the same amount as **A**, **B**, and **C** are accelerated. **E** moves to an energy equal to that of S, mimicking **A**. **D** ends up as low in energy, relative to S, as **C** does high; and thus, proceeds to lag behind as much as **C** leads.

If this beam is left to drift indefinitely, it can be seen that **B**, **C**, and **D** will move arbitrarily far from S. The original bunch will disperse and new ones will periodically appear and fade away.

As drawn, S is special in that the phase coordinate is chosen to move with it and in that it remains un-accelerated. In the initial distribution, however, S was not special at all, except that it (and many other particles) happened to be at the energy chosen as the reference energy. It remained un-accelerated by our arbitrary choice of rf phase. We are free to chose any particle to be our reference particle. S became special by choice. We may even chose a particle which, unlike S up to now, is accelerated. The coordinate system must then simply be redefined so that the energy coordinate, like the time or phase coordinate, tracks with the energy of the chosen reference. The coordinate system is usually defined so as to move with the ideal particle of the beam. That particle, called the synchronous particle, always has the design energy and has a phase relative to the accelerating field so as to maintain that design energy. The energy and time or phase coordinate system, moving with the synchronous particle is called phase space. The coordinates are then $E-E_s$, energy relative to the synchronous particle, and $\phi-\phi_s$, phase relative to the synchronous particle. Particle motion in phase space is then motion relative to the ideal particle. The synchronous particle remains fixed in phase space, changing in energy and advancing in time exactly as desired, simply because that is how it has been defined. The area occupied by the beam particles on the phase space plane is the longitudinal emittance. Usually we are just concerned with the area occupied by one bunch, since we deal with a

periodic system. Typical units for longitudinal emittance, which has dimensions of energy times time, are eV-seconds. In some instances it is useful to transform the vertical axis to momentum, instead of using energy.

As the beam bunch was left in Figure 1D, any particle not on the horizontal axis is destined to move arbitrarily far from S, the reference. This presents no problem if the beam is intentionally left to coast unbunched or if it is on its way to an experiment concerned only with the energy, not the time structure, of the beam. But our intent is to accelerate the beam.

Assume for the moment that S is accelerating. In order that the whole beam accelerate along with it, all particles must "stay close" to S in our phase plane coordinate system. If allowed to move far from S, they are being allowed to become much different from S in time and/or energy; exactly what we do not desire. Nevertheless, with a non-zero energy spread, we cannot completely freeze the motion of all particles relative to S. The beam has a finite emittance, and phase and energy are coupled. The success of our efforts, the stability of the beam, then relies on developing a system to constrain motion to a bounded region of phase space near S.

A hint of the possibility of a stable solution to this problem can be found by imagining the bunched beam in Figure 1D to again be exposed to an accelerating field. If that field is still phased so S sees zero field with a positive slope, it is seen that the higher energy particle C is decelerated, slowing or even reversing its motion away from S. The lower energy particle D is accelerated, bringing its energy closer to that of S and slowing or reversing its motion away from S. Continuing this process, it will be observed that it is possible for particles to travel in "orbits" around S as the drifting and acceleration continues. This action whereby the energy of all particles is focused toward that of the synchronous particle is known as longitudinal phase focusing. The frequency with which a particle "orbits" around the synchronous particle is the synchrotron oscillation frequency. In a circular machine, the number of oscillations per turn (usually much less than one) is the synchrotron tune.

The strength of this focusing action determines the amplitude and frequency of the oscillatory motion relative to the synchronous particle. The amplitude is a measure of how

far in energy or time a stable particle is allowed to travel. The focusing strength is determined by the slope of the accelerating field (the difference in acceleration seen by the synchronous particle relative to another particle at a different phase) and by the rate of time or phase slip between the synchronous particle and another particle with a different energy.

The situation described so far, requires particles with energies greater than that of the synchronous particle to "arrive early", and particles with lesser energies to "arrive late". This is indeed the case for linear accelerators and straight beamlines, since the path traveled by particles is essentially energy independent. In circular machines, the situation is complicated by the fact that, in any given bending field, higher energy particles are bent less than lower energy particles. The higher energy particles, though traveling faster than lower energy particles, follow an orbit with a larger average radius and thus travel a longer path. Which arrives first? At ultra high energies, velocity is essentially the speed of light for all particles independent of small energy differences. In this case, the higher energy particles, having farther to go, actually arrive late. Just the opposite of the situation we started with. At much lower energies the path length and velocity factors compete; and, for each machine, there is some energy for which the effects exactly cancel, the time of arrival is independent of energy. This energy is called the transition energy. Below this energy, higher energy particles do arrive early with respect to lower energy particles.

Remembering that the longitudinal focusing action relied on decelerating higher energy particles and accelerating lower energy particles relative to the synchronous particle, it is noted that the sign of the slope of the accelerating field must be reversed above transition when higher energy particles begin arriving late. This in fact is necessary in machines which accelerate beam through the transition energy. It is accomplished by shifting the phase of the rf by $180°-2\phi_s$, where ϕ_s is the phase of the synchronous particle. The transition energy of a given machine for a given type of particle, E_t, is determined by the circumference and the quadrupole strengths. This energy is usually referred to in terms of the relativistic parameter γ, where $\gamma_t = E_t/m_o$. γ_t is approximately equal to ν_h, the horizontal betatron tune. For example, in the Fermilab Main Ring, γ_t is about 18.7.

The requirement to change the slope of the accelerating field at transition means that the longitudinal focusing strength is changing sign there. For the sign to change (since the focusing strength changes in a continuous manner), the magnitude must pass through zero. The sign change is effectively compensated by shifting rf phase; but the magnitude of the phase focusing strength cannot be prevented from dropping to zero at transition. Since this focusing effect is what bounds motion in the phase space, its disappearance opens the possibility for unbounded motion. Particles are free to move arbitrarily far in time or energy relative to the synchronous particle. Fortunately, any motion in this phase space has a finite velocity, so particles remain near S for some time. In any case, if transition cannot be avoided, loitering in its vicinity should be.

Having constructed the concepts of longitudinal phase space and longitudinal emittance as potentially useful ways of looking at particle beams, how do we relate them to measurable and controllable quantities? There are numerous treatments of longitudinal phase space and motion with any depth of mathematical rigor desired.[1,2,3,4] This paper will stick close to the final results of those efforts without worrying about the derivations beyond the simple intuitive description.

The focusing strength, dependent on the slope of the accelerating field, is a function of the magnitude of a sinusoidally varying rf field of a chosen frequency. It also depends on the difference in time of arrival for particles of different energies, i.e. the drift length (or equivalent) between accelerating cells or the radius of a circular machine. These are real quantities with physical limits for real machines. Finite longitudinal focusing strength implies a finite area of our phase space in which bounded motion relative to the synchronous particle is possible. The obvious limiting case, already discussed, is that in which the beam simply drifts, the rf voltage is zero. The area of bounded motion in phase space, called the bucket area, is then identically zero.

The bucket area also depends on the rate of acceleration. Everything else being equal, the area of a "moving bucket", one in which the synchronous particle accelerates, is less than the area of a "stationary bucket" in which the synchronous particle maintains constant energy. Intuitively, a given rf field has only a limited capacity for affecting a particle's energy. If some of this capacity is used to cause an average

energy change, the capacity for longitudinal focusing is reduced.

For a circular machine, the bucket area is given by

$$S = \frac{8\beta}{2\pi f_{rf}} \sqrt{\frac{2E_s V}{\pi h |\eta|}}\, \alpha(\Gamma) \quad \text{eV-sec} \qquad (1)$$

where β is the relativistic velocity factor; f_{rf}, the rf frequency; E_s, the energy of the synchronous particle in eV; V, the peak rf amplitude in volts; h, the harmonic number (ratio of rf frequency to revolution frequency); and $\eta = (1/\gamma_t^2 - 1/\gamma^2)$, the transition effect factor. γ is simply the particle's total energy normalized to its rest energy. At transition γ equals γ_t and η is identically zero; the bucket area becomes infinite. $\alpha(\Gamma)$ is the moving bucket factor which modifies the bucket area as the synchronous phase is changed. For a stationary bucket, $\phi_s = 0°$, $\alpha(\Gamma) = 1.0$, for $\phi_s = 20°$ $\alpha(\Gamma) \simeq 0.5$, and for $\phi_s = 90°$ $\alpha(\Gamma) = 0.0$. The bucket area depends on the accelerating field amplitude, $S \propto V^{1/2}$, and on the difference in arrival times of particles with slightly different energies, $S \propto (E_s/|\eta|)^{1/2}$.

The maximum momentum spread between the synchronous particle and a particle at the edge of the bucket is

$$\frac{\Delta p}{p} = \pm \left[\frac{1}{cp}\right] \sqrt{\frac{2E_s V}{\pi h |\eta|}}\, \beta(\Gamma) \qquad (2)$$

where cp is the particle momentum in eV units, and $\beta(\Gamma)$ is another "moving bucket" factor depending on the synchronous phase. $\beta(\Gamma) = 1.0$ for $\phi_s = 0.0$, $\simeq 0.5$ for $\phi_s = 35°$, and 0.0 for $\phi_s = 90°$. References 4 and 5 contain graphs and tabulations of $\alpha(\Gamma)$ and $\beta(\Gamma)$.

Particles need not, and frequently do not, occupy the entire bucket area. The bunch area, i.e. the longitudinal emittance, for stable particles is less than or equal to the bucket area. The actual portion of the bucket occupied depends on the energy and time distributions of the particles in the beam. It is these quantities which we must attempt to measure in order to quantify the longitudinal emittance of a real beam. In terms of the time (phase) spread, which can often be measured, the longitudinal emittance is found to be approximately[4]

$$\epsilon_L = \frac{\pi}{16} SQ^2 \left(1 - \frac{5Q^2}{96}\right) \sqrt{\cos(\phi_s)} \quad \text{eV-sec} \qquad (3)$$

where S is bucket area in eV-sec and Q is the peak phase excursion of any particle relative to ϕ_s. Q is 1/2 the total phase spread, in radians, (peak bunch length) of the beam. This expression is accurate to about 6% for beam filling a stationary bucket. The approximation deteriorates for large synchronous phases and for large amplitude motions, i.e. bunch areas comparable to the bucket area.

The rate at which particles "orbit" around the synchronous particle in phase space, the synchrotron frequency, is given by

$$f_s = \frac{f_{rf}}{\beta} \sqrt{\frac{|\eta| V}{2\pi h E_s} \cos(\phi_s)} \left[1 - \frac{Q^2}{16}\right] \text{ hertz} \qquad (4)$$

where all quantities have been previously defined and E_s has units of eV. The last term accounts for the fact that the frequency is somewhat amplitude dependent; that term is, in fact, only an approximation, correct for small amplitudes. Notice that the η term is contained in the numerator, forcing the oscillation frequency to zero at transition. Note also that bucket area, emittance, and synchrotron frequency all scale as the square root of the rf voltage.

It should be realized that no real particle need be identical to the ideal synchronous particle. Particle distribution in phase space is not necessarily uniform nor symmetric about the synchronous particle. Figure 2 shows some possible distributions in phase space and the projection of those distributions on the time axis. The synchronous particle is at the origin of each plot and the buckets are assumed stationary. Evolution of each distribution is followed for one half synchrotron period. The first distribution, uniform and symmetric around the synchronous particle, appears stationary though individual particles circulate around within. The second distribution represents a bunch whose centroid begins with a phase or timing error. The time projection maintains a uniform shape, but oscillates back and forth relative to the synchronous phase. The last distribution has an asymmetric aspect ratio such that at one phase of the motion the particles are grouped tightly in phase with a large

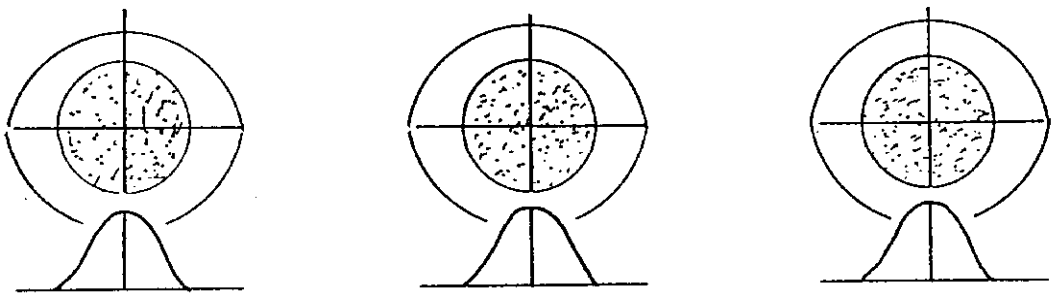

A. Symmetric and centered

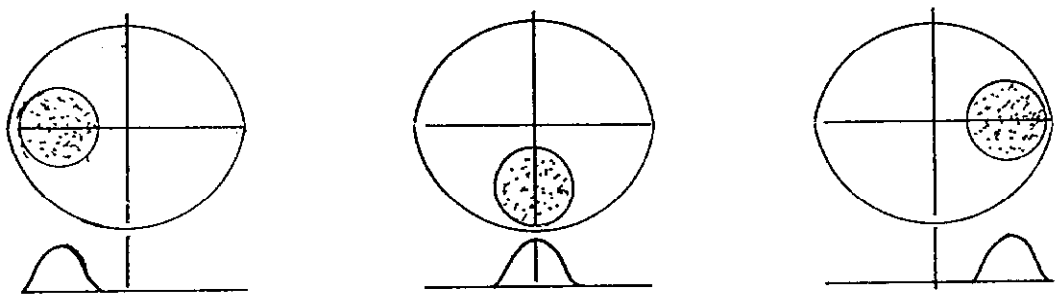

B. Symmetric and off-center

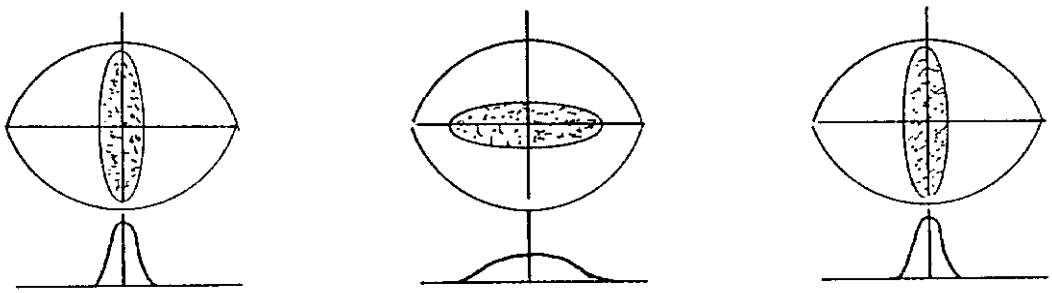

C. Asymmetric and centered

FIGURE 2
POSSIBLE PARTICLE DISTRIBUTIONS AND THEIR EVOLUTION IN A BUCKET

energy spread, and 90° later the energy distribution is reduced at the expense of increased time spread. Any combination of these and higher order mode distributions are possible.[6]

Bucket area must be sufficiently large to contain all particles of interest at any phase of their motion in order to maintain stability. The emittance of the beam must be considered as the entire phase space area covered and/or enclosed by the particles during one complete oscillation, not just the area they happen to occupy at any instant of time. The last two distributions in Figure 2 are examples of beam mismatched to the bucket. Such mismatches are generally undesirable because the effective momentum spread of the beam is increased and loss of particles may result. Mismatches result in an inefficient use of bucket area since more rf voltage, and therefore more power and money, is required to contain the beam than would be necessary in a matched condition.

The time projections of the phase space beam distributions begin to take on real significance to the engineer when it is realized that what is being considered is a time distribution of charged particles moving through space. This is simply an electric current which can be measured to yield the time or phase distribution of the particles in the beam.

MEASUREMENT METHODS

Techniques of measuring particle energies and time distribution rely on only a few fundamental physical principles, including the radiation of and interaction with electric and magnetic fields by charged particles, and the relationship between velocity and energy. The ways in which these principles have been exploited are innumerable. Methods used depend on many variables -- What is the availability of the beam? Single pass or circulating? May the measurement be destructive of the beam? What is the energy range of the particles? What time resolution is required? What spatial resolution is required? What type of particle is to be measured? What is the end use of the information? And so on... A few examples will be presented.

ENERGY MEASUREMENT

THE SPECTROMETER

The fundamental spectrometer technique relies on the ability to subject the beam to energy dependent forces and monitor subsequent motion. A classical spectrometer is sketched in Figure 3. An example exists at the end of the Fermilab 200 MeV Linac. All or a portion of the beam is directed through a magnet, which introduces a bend angle[5]

$$\theta = \frac{L}{\rho} \tag{5}$$

where L is the magnet length, and ρ is the radius of curvature of the particle path in the field B.

Since

$$B\rho = \frac{p}{q} \tag{6}$$

find

$$\theta = \frac{BLq}{p} \tag{7}$$

where p is the particle momentum and q its charge.

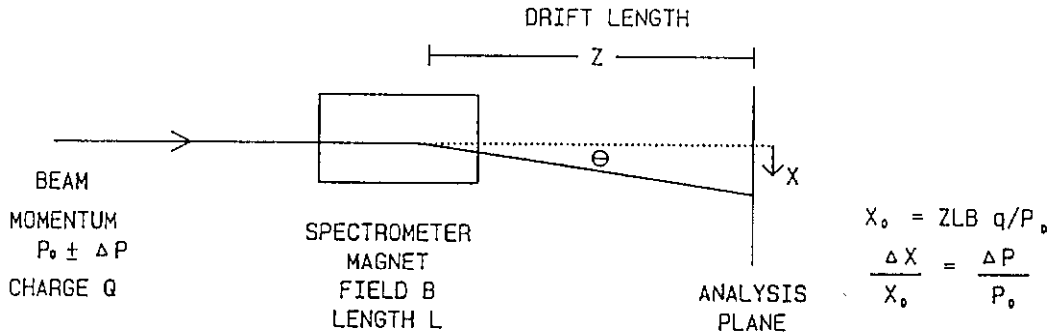

FIGURE 3
TYPICAL SPECTROMETER SETUP

Some distance z downstream, a particle of momentum p will be displaced by

$$x = \frac{zBLq}{p} \tag{8}$$

The spread in energy of a beam with a central momentum p_o is found from

$$\Delta x = \frac{-zBLq}{p_o} \frac{\Delta p}{p_o} = -x_o \frac{\Delta p}{p_o} \tag{9}$$

$$\frac{\Delta x}{x_o} = \frac{\Delta p}{p_o} \tag{10}$$

The fractional displacement spread is equal to the fractional momentum spread.

Note that this treatment assumes that all particles enter the spectrometer magnet with the same angle and at the same position, that is, it assumes zero transverse emittance. A real beam has finite transverse emittance. The contribution of this emittance to the position spread at the observation point must be accounted for to obtain a correct momentum spread measurement. Either, the momentum sensitivity of the position is made so large as to overwhelm position spread due to transverse beam size; the measurement is made at one location for different known transverse focusing conditions; or, the the beam is observed at more that one spot in a beamline with known optics so that the transverse effect can be calculated out.

At Fermilab the beam is observed at one location using a single wire which may be scanned in position across the beam. At any wire location, the charge deposited on the wire by the beam by secondary emission effects is electronically integrated to provide a signal proportional to the amount of beam intercepted. A histogram of beam density vs. position thus generated can be interpreted as a momentum distribution plot.

Circular accelerators or storage rings are effectively continuous spectrometers. Any ring has a dispersion function[2], determined by the transverse focusing optics, of some value at any location. The dispersion function, D, relates the radius of the particle orbit to its momentum, $\Delta R = D(\Delta p/p)$. This effect has been used in the Fermilab

Tevatron to measure momentum spread and calculate longitudinal emittance. The horizontal beam profile is measured at two locations where the dispersion is different and the transverse lattice functions are known. These profiles contain the information necessary to de-convolve transverse and longitudinal emittance contributions. Beam profiles are measured with "flying wire" monitors[6]. Another aspect of the "continuous spectrometer" appears in frequency domain measurements when the effect of momentum on revolution time is considered. This aspect will be discussed later.

A spectrometer scheme is also used to measure the energy spread of the e^+ and e^- bunches in the SLAC Linear Collider.[7,8,9,10,11,12] The magnet which splits the electrons and positrons into their respective transport lines to the collision point is used as the spectrometer magnet. The energy spread of the beam and the dispersion introduced by this horizontal bend combine to produce a spread in the horizontal beam size at some distance downstream where the beam passes through the vertical wiggler magnet to induce synchrotron radiation. The horizontal width of the radiation source is the same as the beam size and therefore directly related by the dispersion to the momentum spread. The synchrotron radiation shines on a phosphor screen viewed by a TV camera. The TV image is digitized and processed to produce an energy histogram. Separate systems measure each of the two beams, positrons and electrons. The absolute energy of the beams is measured by sensing their centroid positions in the high dispersion regions using stripline beam position monitors. The results of this measurement provide important real-time feedback to the linac to stabilize the energy.

TIME OF FLIGHT MEASUREMENTS

The energy of any particle may be determined from its velocity if its rest mass is known. The velocity can be calculated if the time required to travel between two points along a known path is measured. Energy determinations can be made quite sensitively using this method for particles with velocities much less than $\beta = 1$. As particles become relativistic the slope of the velocity vs. energy curve approaches zero, as does the sensitivity of this energy

measurement technique. Two examples of this technique are presented.

The Fermilab Linac is in the midst of an upgrade project to replace the four high energy tanks with new side-coupled accelerator structures to increase the Linac output energy from 200 MeV to 400 MeV. To insure optimal performance, the energy gain per cell and the phasing between cells must be correctly adjusted. A method of measuring the energy gain as a function of rf amplitude and phase, based on schemes from Los Alamos[13,14], has been implemented on several existing linac tanks in preparation for this effort. The beam comes in a 30μsec pulse bunched by the 200 Mhz rf. Beam signals are available from stripline pick-ups located at each end of each tank. Signals from the upstream and downstream end of the tank of concern are compared by an electronic phase detector circuit. Phase comparison of signals of a known frequency is equivalent to a time measurement. As the rf amplitude and phase is adjusted, the phase between the upstream and downstream beam signals can be monitored. Interpreted as a change in time of flight between the two striplines, the energy gain of the beam within the tank can be computed. This method has proven successful and has already demonstrated the existence of matching errors between tanks in the existing linac.

H^- beams from the ATS (Accelerator Test Stand) radio frequency quadrupole (RFQ) accelerator at Los Alamos are analyzed in energy using time of flight techniques.[15,16] Laser

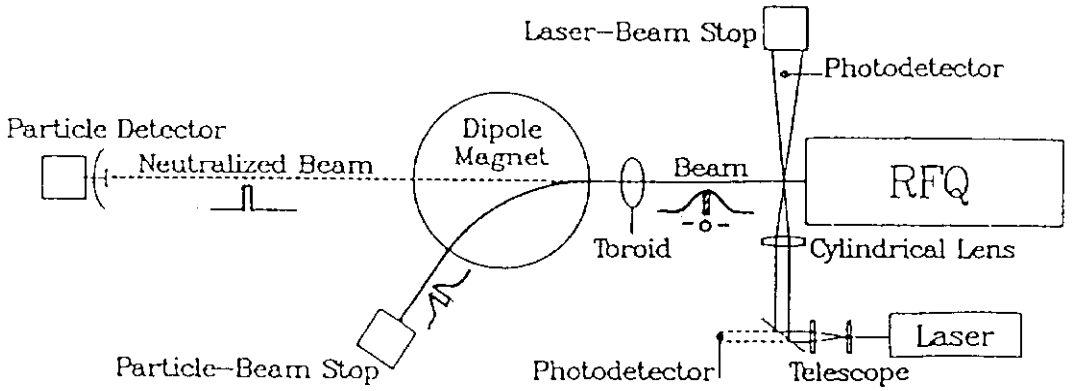

FIGURE 4
LOS ALAMOS ACCELERATOR TEST STAND
LASER-INDUCED NEUTRALIZATION DIAGNOSTIC APPARATUS
(figure taken from ref. 15)

induced neutralization is used as a means of sampling a short time segment of an H^- bunch from the RFQ. See Figure 4. A 32 picosecond laser pulse is focused to a 30 micron diameter and shined on the beam, perpendicular to the direction of beam travel. The laser energy strips one electron from the H^- ions, creating a neutral beam from a 200 micron slice of the bunch's longitudinal dimension. A dipole magnet sweeps away remaining charged particles while the neutral segment travels straight ahead to a fast secondary emission monitor (SEM). Detection of the laser light by a fast photodetector initiates the timing interval which terminates when beam arrives at the SEM. For the known drift length and measured time interval, the energy of the particles can be calculated. The timing of the laser pulse is measured relative to the phase of the RFQ rf. This information and the ability to sample only a small fraction of the bunch length allows measurement of particle energy as a function of rf phase. Integration of the signal from the neutral particle detector provides the information necessary to determine particle density vs. phase. It is thus possible to measure the complete longitudinal phase space parameters of the beam.

BUNCH SHAPE AND TIME DISTRIBUTION MEASUREMENTS

The Los Alamos laser induced neutralization scheme demonstrates that particle time distribution can be determined by arranging to tag a small time slice of the bunch and sample only the tagged particles. Few situations allow the slick technique of altering the charge state of a slice of beam, but other implementations of sampling techniques are possible. These methods usually rely on the transformation of temporal distribution to spatial distribution.

Two such examples involve processing the beam of secondary electrons generated from a wire or foil target intercepting the beam to be measured. A method developed at Brookhaven[17], Figure 5, modulates an acceleration voltage applied to the secondary electron beam in synchronism with the rf of the primary beam. The energy modulated electron beam travels through a region of uniform magnetic field. The momentum spread of the electron beam is transformed to a spatial spread on a plane where each electron has

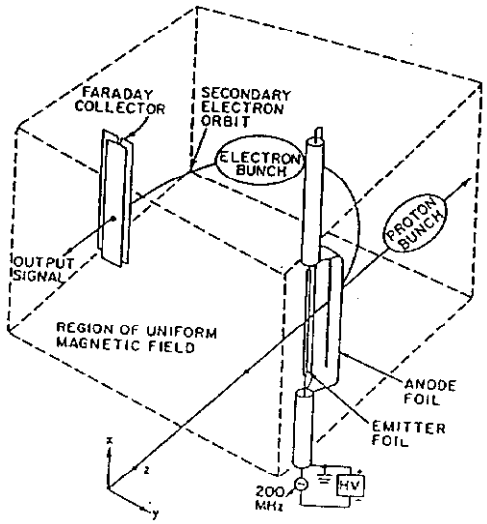

FIGURE 5
BROOKHAVEN BUNCH LENGTH MONITOR
(figure taken from ref. 17)

completed one half of a circular path in the magnetic field. A Faraday cup charge collector with a narrow entrance slit placed on this plane provides a signal from only those secondary electrons with the "right" energy, that is, those due to particles in the primary beam at a time when the electron accelerating voltage is at a particular value. By varying the phase of the electron accelerating voltage relative to the bunch, the "right" accelerating voltage is moved in time relative to the bunch. Thus, the charge measured at the Faraday cup is a representation of a particular time sample of the original beam.

A modification of this scheme, developed at INR in the USSR, Figure 6, accelerates all secondary electrons to the same energy.[18] This electron beam is then passed between a pair of deflecting plates driven with an rf voltage synchronous with the beam rf. The position of these particles some distance downstream becomes a function of the time at which they were deflected. Since this beam has the same temporal distribution as the primary beam, that distribution is effectively transformed to a spatial distribution, the position of which may be translated by adjusting the phase of the deflecting voltage. Again, a Faraday charge collector with a narrow entrance slit samples a small part of the spatial distribution to provide an electrical signal. Time resolution the order of 1° at 600Mhz is reported. Bunch shape

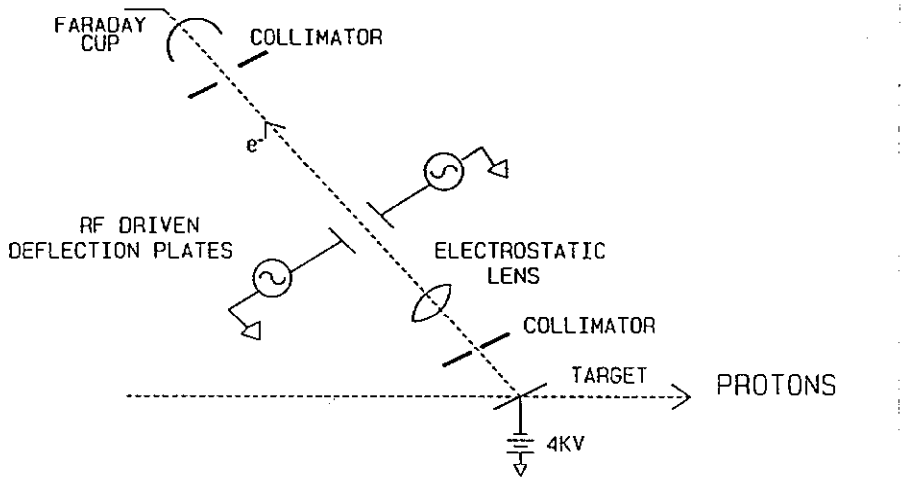

FIGURE 6
USSR INR BUNCH LENGTH MONITOR SCHEME

measurements by this device under different conditions of the primary beam have allowed calculation of longitudinal emittance values for the beam.

Bunch shape measurements have been made at the Daresbury Synchrotron Radiation Source using synchrotron light focused onto an image dissector tube.[19] The front end of the image dissector tube consists of a photocathode. Photoelectrons produced there have essentially the same time distribution as both the synchrotron light and the original electron beam which is desired to be measured. In the image dissector tube, the photoelectrons are accelerated and operated on by a transverse deflection scheme similar to that just described. The Faraday cup is replaced by an electron multiplier dynode structure with a slit entrance aperture. Transit time spread of electrons through the multiplier limits the time resolution of this device.

At SLAC, Cherenkov light from a radiator positioned to intercept the electron beam is focused onto a streak camera.[20] The streak camera is another device utilizing photoemission and fast electron deflection to transform a high speed time image to a spatial image which can be electronically processed. Streak cameras are also used at Orsay to measure time duration of picosecond electron bunches.[21]

Where time resolutions of picoseconds are not required,

various types of current transformers are generally used for bunch shape measurements.[22,23,24,25] One such type of transformer is the "wall current monitor".[26,27,28] This type of device can offer bandwidths of several gigahertz. A wall current monitor is described in detail later in this paper.

Applied to beams in beamlines or linacs, current monitor signals are generally processed by oscilloscopes (which still rely on the ability to transform time into position by the deflection of electrons). These may be conventional analog scopes, sampling scopes, or one of the growing number of high speed digitizing sampling scopes. Where the sampling rates are too slow in real time, interlaced sampling using external triggering synchronized to the accelerator rf allows a bunch profile signal to be built up over many pulses. Thus the full risetime bandwidth of the sampling head may be realized, subject to any jitter in the triggers. These techniques are, of course, applicable also to signals from current monitors in circular machines.[29] All result in direct time domain representations of bunch shapes.

An ever increasing number of video and image processing techniques and technologies are available for capturing, archiving, and analyzing bunch shape information that can be displayed on oscilloscope screens. These include video frame grabbers, video image tape recording, etc. For instance, beam bunch signals, as viewed on a scope screen by a video camera, are routinely recorded by a standard VCR during antiproton acceleration cycles and transfers when Fermilab operates in the collider mode. This provides a record in the event it becomes necessary to autopsy a doomed antiproton injection or acceleration cycle.

Beam bunch signals from circular accelerators are frequently presented in the form of mountain range displays, e.g. Figure 7. Such displays are generated by adding the beam current signal to a slowly increasing voltage ramp or staircase. The resulting signal is displayed on an oscilloscope triggered synchronously with the accelerator rf. Multiple triggers during the slow voltage ramp, result in a family of traces offset in vertical position on the scope screen. Thus, the time evolution of a fast bunch signal can be monitored and displayed in a single picture. The delay between each trace of the family can be made arbitrarily long by adjusting the repetition rate of the rf synchronous triggers and the slope of the slow ramp. This is simplified with a two channel scope that allows addition of the signals from the

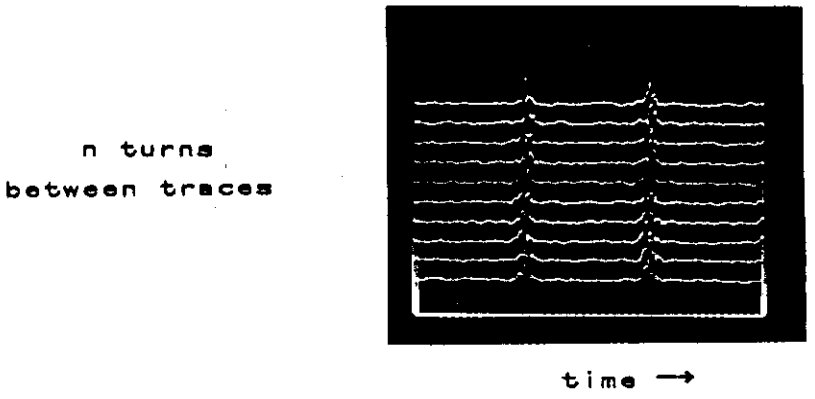

FIGURE 7
TYPICAL MOUNTAIN RANGE DISPLAY

two channels. This type of display facilitates the observation of bunch phase oscillations (synchrotron oscillations of the centroid of the bunch), bunch shape oscillations, and special bunch manipulations such as bunch coalescing used in the Fermilab collider. Even intrabunch momentum oscillations can be observed if the difference signal from a position monitor in a high dispersion region is viewed on this type of display.[30]

If the signal from a fast beam current monitor is used to trigger a sample of the machine rf waveform, bunch phase oscillations can be measured without the need for a mountain range display or wideband scope. This circuit is essentially a type of phase detector. Variations of the sampled output indicate beam motion in time relative to the rf.

Bunch shape oscillations of the type shown in the third beam distribution of Figure 2 are easily observed by peak detection (e.g. by a diode) of a fast beam current signal. The resultant signal may be observed on low bandwidth equipment. Signals processed in this manner have been used to provide stabilizing feedback to beams in synchrotrons.

FREQUENCY DOMAIN INFORMATION

In recent years much attention has been given to frequency domain interpretation of signals from beam monitors

in circular machines.[30,31,32] Several treatments with varying degrees of mathematical rigor are available. A few results and applications will be mentioned here.

An unbunched beam circulating in a synchrotron or storage ring will produce signals in a current monitor at all multiples of the revolution frequency. This is a consequence of the quantum nature of the particles and their random distribution around the machine. In this sense, the signal is like the shot noise associated with, for instance, currents in an electron tube. These random signals are called Schottky signals and are proportional to the square root of the number of particles. Since particles of different momenta in the unbunched beam are free to circulate at correspondingly different revolution frequencies, each makes a signal contribution at its own frequency. Consequently, the spectrum of the Schottky signal has a characteristic width at each revolution harmonic directly proportional to the momentum spread of the beam and the harmonic number. This effect allows rather easy determination of the energy spread of a circulating beam. The signal from a current monitor is simply displayed on a spectrum analyzer. Scaling is

$$\frac{\Delta f}{f} = -\eta \frac{\Delta p}{p} \tag{11}$$

Schottky signal currents are quite weak since they scale with the square root of the number of particles, rather than linearly. For this reason, beam pickups to sense the Schottky signals area generally designed to be relatively narrowband tuned pickups, as opposed to wideband devices like the wall current monitor. Wideband devices typically present only a few ohms impedance to the beam, whereas tuned devices are easily constructed to present the beam with kilo-ohms. Since signal power is proportional to this impedance, the advantage is obvious. The momentum spread of beams in antiproton accumulator rings is usually measured by this technique just described.[33] Longitudinal stochastic cooling relies on Schottky signals.[34]

Bunched beams, on the other hand, by definition consist of particles which on the average have exactly the same revolution frequency as all other particles in the beam. This average frequency is controlled by the rf system which maintains the bunch by its phase focusing action. A particle, which may at one instant of time have a higher frequency

than the synchronous particle, must at some later time, have a correspondingly lower frequency in order to remain part of the bunch. The result is that the bunch now creates coherent signals with a predictable time structure, i.e. the pulse in time we recognize as the bunch shape. If the bunch shape is known, the spectrum of the periodic bunch signal can be calculated as a Fourier series without resorting to statistical methods as is necessary for the Schottky signal.

The Schottky signals do not, of course, cease to exist. The beam still consists of quantized charges with some randomness of distribution within the bunch. The longitudinal Schottky signals appear as fm sidebands around each harmonic of the revolution frequency. The revolution harmonic is arbitrarily narrow for fixed rf frequency, while each fm sideband signal has a finite width related to the momentum spread. The appearance of fm type sidebands due to the variation of individual particle revolution frequencies around the synchronous frequency can be appreciated if compared to an rf communication signal in which the instantaneous signal frequency is varied around a central frequency. The fm sideband components are displaced from the corresponding revolution harmonic signal by multiples of the synchrotron oscillation frequency. Since the synchrotron frequency is generally small compared to the revolution frequency, the fractional frequency separation between the strong coherent revolution harmonic signal and the weak incoherent sideband is very small. Recovery of longitudinal information contained in an fm sideband requires a specially designed narrowband receiver. There are usually easier ways to acquire desired information from bunched beams.

One such method to derive bunch length information by processing coherent frequency domain signals from a beam current monitor or appropriate stripline monitor is used at Fermilab.[35] The technique begins with the assumption of an appropriate bunch shape model, in this case gaussian. The Fourier signal components required to represent such a bunch, periodic at the revolution frequency, are then computed as a function of the rms bunch length. The sensitivity of different spectral components to changes in bunch length is determined and two components with adequate sensitivity are selected. In the Fermilab application, the selected frequencies are the first and third harmonics of the rf frequency. Frequency selective receivers detect the amplitude of these components and an analog circuit computes the bunch length. The

bunch length is proportional to the square root of the natural logarithm of the ratio of the two spectral amplitudes. A real time bunch length signal, with 10 Khz bandwidth, is thus generated for use as a beam feedback signal or simply as a diagnostic tool.

This survey represents only a few of the methods that have been used to get a handle on the quantitative aspects of particle beams related to their longitudinal emittance -- energy, energy spread, and bunch shape. In addition to the many references cited here, the Particle Accelerator School publications offer introductory descriptions to many topics and the Particle Accelerator Conference Proceedings provide a wealth of technical detail.

A WALL CURRENT MONITOR

Knowledge of the time distribution of particles in a beam is important for assessing the performance of an accelerator and for monitoring its operation. To this end, a device for measuring beam current with flat amplitude response and the best possible time resolution is essential. The words "broadband current transformer" could generically describe a device with the desired characteristics. A simple current transformer is depicted below in Figure 8.

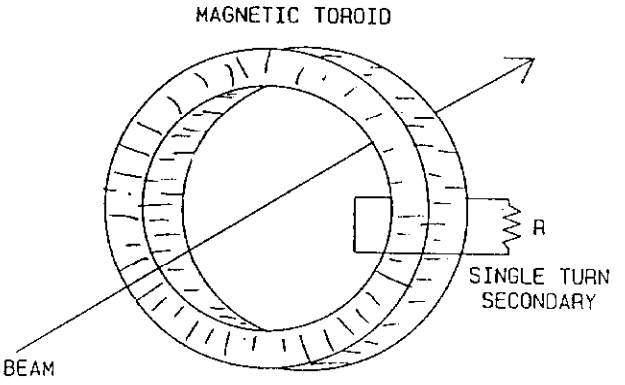

FIGURE 8
SIMPLE CURRENT TRANSFORMER

The response of this device is easily calculated observing that the magnetic flux in the core is equal to the sum of that resulting from the beam current and that resulting from the current in the secondary winding. Assuming a single turn secondary, we have

$$\Phi_T = \Phi_b + \Phi_s = Li_b + Li_s \tag{12}$$

where L is the inductance of any single turn winding on the magnetic toroidal core.

$$L = \frac{\mu\mu_0 h}{2\pi} \ln \frac{b}{a} \tag{13}$$

where h is the core thickness and a and b are respectively the inner and outer diameters of the core.

Faraday's law of induction tells us that the induced current i_s will be of a polarity so as to oppose the flux due to i_b. Noting this and that the induced voltage in the secondary is equal to the rate of change of total flux we write

$$\frac{d\Phi_T}{dt} = v_s = L\frac{di_b}{dt} - L\frac{di_s}{dt} \tag{14}$$

Substituting $v_s = i_s R$ and switching to frequency domain notation we find

$$V_s(\omega) = j\omega L I_b(\omega) - j\omega L \frac{V_s(\omega)}{R} \tag{15}$$

Solving for V_s

$$V_s(\omega) = j\omega L \frac{I_b(\omega)}{1+j\omega L/R} \tag{16}$$

This is the response of a high pass filter with a 3db point at $\omega_c = R/L$ and a passband transfer function $v_s = i_b R$.

The transformer effectively forces a current equal to the beam current through the load resistor. The current is measured by measuring the voltage across the load. This is good for frequencies above $f_c = \omega_c/2\pi = R/2\pi L$. Notice that there has been no requirement for any "wall" currents in any beam tubes and the low frequency corner can be made arbitrarily small.

Now, change the geometry of the original picture without changing the effective circuit. Rotate the secondary winding so the resistor appears inside the core, then revolve the whole secondary about the longitudinal axis of symmetry. The core is now surrounded by a metal housing except for a uniform resistive gap in the inner diameter. A cross section is shown in Figure 9.

A beam tube may be added to each end of the transformer without changing the circuit response, which is determined solely by the gap resistance and the inductance presented by the core. The beam tube can even close upon itself and have numerous grounds without affecting the signal because these paths are now simply in parallel with the arbitrarily low resistance of the housing. See Figure 10. The housing also shields the resistive gap from external signal sources. At dc, the attenuation of external signals is simply the ratio of the housing resistance to the gap resistance. For ac signals, the attenuation is further enhanced, as the inductance presented by the core appears in series with the gap resistance. Finally, at rf frequencies, the skin effect prevents any external signal from reaching the gap.

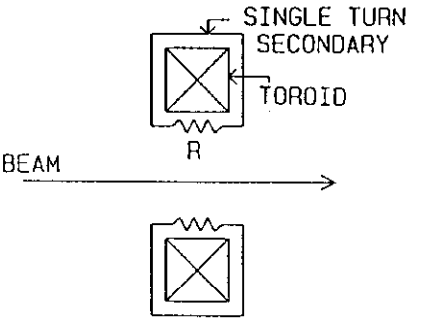

FIGURE 9
SIMPLE TRANSFORMER
NEW GEOMETRY

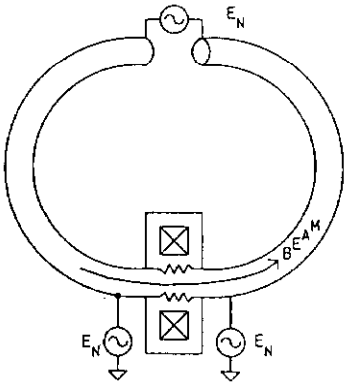

FIGURE 10
TRANSFORMER IN
ACCELERATOR

One further mechanical modification

and the addition of a gap voltage monitor tap completes the initial conceptual design of the monitor. The mechanical modification is the addition of a ceramic vacuum seal between the beam and the gap resistance, allowing the resistance and the magnetic material to reside outside the vacuum. The ceramic is not necessary if the vacuum properties of the material are adequate for the application. However, the trend toward ultrahigh vacuums, especially in storage rings, makes the use of the ceramic seal generally advisable. Half the cross section now appears as shown in Figure 11.

FIGURE 11
HALF CROSS-SECTION OF
PHYSICAL TRANSFORMER

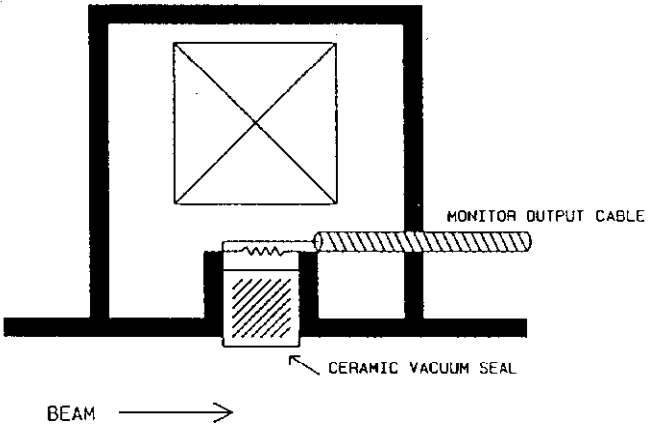

A beam current transformer has thus been developed, but at least two questions remain open -- What happened to the wall current monitor concept, and what limits the high frequency response?

The electric and magnetic fields due to the beam are properly thought of as electromagnetic waves propagating out from the beam. At low frequencies, the magnetic component of the wave penetrates the metallic walls of the beam tube and the transformer. This is how the flux can appear in the magnetic core of our transformer. In fact, the dc component of a beam current totally enclosed within a conducting nonmagnetic pipe can be measured external to the pipe without the need for any type of insulating break in the pipe. The dc magnetic field exists external to the pipe and can be measured, for example, with a second harmonic type dc transformer.

At higher frequencies, the wave is attenuated as it propagates through the conducting beam tube -- the skin effect. At high enough frequencies, where the skin depth is

a fraction of the wall thickness, the attenuation is effectively complete. No high frequency field appears external to the beam tube. The only way for the fields due to the beam currents to not appear in some region of space is for them to be exactly canceled by equal and opposite fields due to some other current distribution. Since the beam fields appear within the beam tube, but not outside of it, the cancelling fields must be generated by currents in the wall of the tube. At last, the long lost wall currents! So the idea of a wall current monitor is seen to be correct at frequencies where the skin depth in the wall is small. The idea of wall currents can also be introduced intuitively by considering that a bunch of beam electrically induces an opposite charge in the beam tube. As the beam bunch moves, so too must the induced wall charge; hence, wall currents.

To see these currents, it must be arranged for the resistor to appear in series with the wall. What foresight, that's just where it was last left in Figure 11. The effect of wall currents equal and opposite to the beam flowing through the resistor is identical to the effect of the low frequency transformer forcing a current equal and opposite to the beam through the resistor. There is no "cross-over" problem, only a change in point of view.

The idea of wall currents allows consideration of bandwidth limitations of the monitor in terms of circuit models. The impedance through which this wall current must flow as it passes the monitor is the parallel combination of the impedances presented by the physical gap, the intended resistance with its strays, and the surrounding volume loaded with magnetic and possibly other material. The voltage to be measured and related to the beam current is that due to the portion of the wall current which flows in the intended resistance. Therefore, it must be insured that all or at least

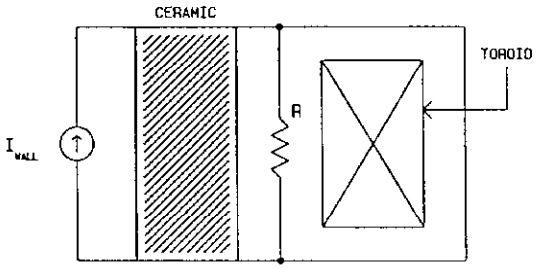

FIGURE 12
WALL CURRENT MONITOR
CIRCUIT MODEL

a constant fraction of the wall current follows that path rather than a parallel path. The circuit can be modeled as in Figure 12. It looks amazingly like the mechanical sketch of Figure 11 rotated 90°. Keeping in mind the goal of insuring that a large constant fraction of the current flow through the resistor, the requirements of each component can be studied.

Begin with the cylindrical outer volume, partially filled with magnetic material. It forms a cylindrical cavity, presenting some shunt impedance across the resistor. This impedance ought to be made large relative to the resistance at all frequencies of interest; if not ignorably large, at least relatively constant. At low frequencies, the impedance is simply the single turn winding inductance, chosen to set the low frequency L/R time constant. At higher frequencies, determined by the magnetic material, the cavity exhibits appreciable loss. The shunt inductance begins to look more like a resistor; still OK if the value is large compared to the gap resistance. The shunt impedance of the cavity at moderate frequencies increases linearly with the number of cores. This number may be increased as space permits. At some high frequency, electromagnetic waves impinging on the surface of the material will not penetrate; they will be reflected with little attenuation. At this point the material does little good except to define the boundary of a now smaller cavity which may resonate and present a low impedance across the resistance at some frequencies. Different additional material may be added to handle frequencies in this range.

This graded approach was chosen for our design, filling the volume with several different materials. Farthest from the gap are Ceramic Magnetics, Inc., MN60, manganese-zinc ferrite cores with $\mu \simeq 6000$. Four of these cores with dimensions 4" i.d., 6" o.d., and 1" high provide a low frequency inductance of about $40\mu H$ and a broadband resistance of $\simeq 20\Omega$ in the ten to hundred Mhz range. Closer to the gap, two Ceramic Magnetics C-2025 ferrite cores, $\mu \simeq 175$, provide loss to higher frequency signals, attenuating them before reaching the MN60 which becomes less useful at these frequencies. Closer yet to the gap are two epoxy cores loaded with microwave absorbing material. The remaining volume near the gap is filled with a foam type microwave absorbing material. The inner wall of the cavity is coated with a microwave absorbing paint to further damp any

surface currents induced by waves managing to find their way to the walls. Indeed, the object is to make this volume appear as a black box into which energy enters, as into a high impedance, and is totally absorbed. Our design results in a broadband impedance of between 10 and 20 ohms up to multi-gigahertz frequencies. This effective cavity shunt impedance dictates a choice of around one ohm for the gap resistance, in order to limit the shunting effect to about 10%.

Satisfied with minimizing the cavity effect, the circuit simplifies to that shown in Figure 13. Pessimistically, the ceramic section can be modeled as a lumped capacitance which sets the high frequency rolloff of the device at $\omega = 1/RC$. Taking a more optimistic point of view, the ceramic can be seen to form a radial transmission line (a distributed rather than a lumped element circuit) through which currents from the inside of the beam tube must flow to reach the monitoring resistor. If the resistor terminates this line in its characteristic impedance there is theoretically no frequency sensitivity.

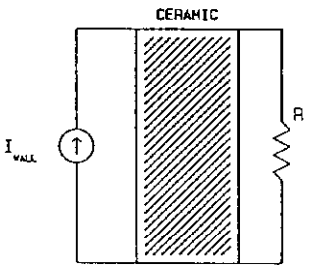

FIGURE 13
WALL CURRENT MONITOR
SIMPLIFIED CIRCUIT MODEL

To estimate the characteristic impedance of this radial line, look from the inside of the beam tube radially outward and unroll the cylinder to a plane. The gap then simply looks like a parallel plate transmission line with a plate separation equal to the gap width and plate width equal to 2π times the radius at which the ceramic resides. The impedance of such a line is

$$Z = 377 \frac{h}{w} \frac{1}{\sqrt{\epsilon_r}} = 377 \frac{h}{2\pi R} \frac{1}{\sqrt{\epsilon_r}} \qquad (17)$$

where ϵ_r is the dielectric constant of the ceramic filling the volume between the plates. For our gap, r $\simeq$ 1.75", h = 0.125", and $\epsilon_r \simeq 9.5$. The radial line impedance is found to be 1.4Ω. This ceramic section was made to our specifications

to match the previously determined magnitude of the gap resistance, about one ohm. The radial extent of this line is basically the wall thickness of the ceramic, in our case, 3/16". The high dielectric constant slows the radial wave propagation, effectively making the line look longer by $\sqrt{\epsilon_r} = 3$. The circuit now is as shown in Figure 14.

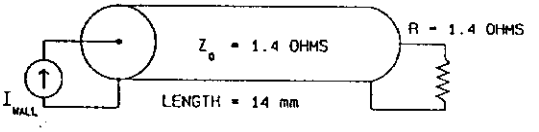

FIGURE 14
TRANSMISSION LINE MODEL

Some validity to assuming the radial line point of view is lent by the data in the Figure 15. It shows measurements made on a wall current monitor of a previous design, exhibiting a ≃20db peaking in the frequency response. In an attempt to explain this undesirable response, the radial transmission line model was applied. The radial line impedance for that ceramic geometry was calculated to be approximately 3.2 ohms. The resistance of the device was 0.32 ohms. The length of the radial line corresponded to one quarter wavelength at 1.9 Ghz, the same frequency at which the peaking was observed. Response of a Spice program model of a current source driving that transmission line and termination agrees with the measured resistor voltage over the full range of measurements.

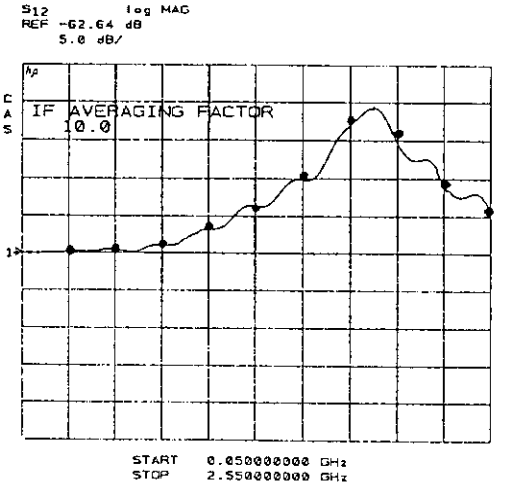

FIGURE 15
RESPONSE OF MONITOR WITH
MIS-TERMINATED RADIAL LINE
MEASURED (solid)
PREDICTED (dots)

With an understanding of the surrounding cavity shunt impedance and the radial transmission line model in hand, consideration of the resistance itself and connection of a suitable voltage monitor remain. A distributed resistance is appropriate since other parts of the monitor are treated as distributed transmission lines. We use 80 120Ω rf chip resistors evenly spaced around the circumference. These resistors are used because they exhibit very high self-resonant frequencies, i.e. they really act as constant value resistors over the frequency range of concern. The resistors are soldered to metal bands on either end of the ceramic gap and are kept close to the outer surface of the ceramic. This provides approximately the required 1.4Ω resistance with good high frequency characteristics.

Design of a voltage monitor requires an understanding of the voltage distribution around the circumference of the gap. This voltage may properly be considered as the linear superposition of two contributions: 1) a sum or average gap voltage (the zeroth order term in a harmonic expansion of the azimuthal voltage distribution), and 2) a difference voltage (all higher order terms in the harmonic expansion).

Only energy propagating outward through the radial transmission line contributes to the sum voltage. The difference voltage, on the other hand, results only from energy propagating azimuthally around the gap. It is important to realize that these two paths are different from each other, with grossly different propagation constants. The radial line, properly terminated, will transmit the sum signal with little attenuation, producing a sum signal voltage at the resistors independent of frequency (above the low frequency L/R corner). To azimuthal waves, the gap looks like a parallel plate type transmission line with a plate width corresponding to the wall thickness of the ceramic and a plate separation corresponding to the gap width. This line is filled with ceramic dielectric and heavily shunt loaded by the intended gap resistance. The result is a lossy line with frequency dependent characteristics.

For centered beam, only the sum signal (i.e. the radial mode) exists, the voltage distribution is uniform by symmetry. There is no azimuthal transfer of energy and the gap voltage has no fundamental upper frequency limit. The often cited $1/2\pi RC$ limit is simply incorrect if the radial line mode is properly terminated. For off-center beam, the voltage at any point around the gap is the superposition of

the frequency independent sum component and a frequency dependent difference component. The difference component sees a driving source determined by the beam position and bunch shape, and displays a frequency dependence determined by the azimuthal line parameters.

For our gap, we find azimuthal line parameters as below:

capacitance	--	3 pf/inch
inductance	--	21 nh/inch
conductance	--	0.071 mho/inch
series resistance	--	$\simeq$ 0 Ω

The capacitance is simply the total gap capacitance divided by the circumference. The inductance is found by considering the line without the shunting resistors. It is a line with dielectric constant $\epsilon \simeq 9$ and known capacitance per unit length, C. The propagation velocity is then $c/\sqrt{\epsilon}$, where c is the speed of light. We have

$$v = \frac{c}{\sqrt{\epsilon}} = \frac{1}{\sqrt{LC}} \tag{18}$$

$$L = \frac{1}{C} \cdot \frac{\epsilon}{c^2} \tag{19}$$

The conductance is the total gap conductance (the inverse of the gap resistance) divided by the circumference.

The line propagation constant is defined

$$\gamma = \sqrt{(R+j\omega L)(G+j\omega C)} \Rightarrow \sqrt{j\omega L(G+j\omega C)} \tag{20}$$

For $G >> \omega C$, ($f << 3.8$Ghz), we can approximate

$$\gamma \simeq \sqrt{j\omega LG} = \sqrt{\omega LG/2}\ (1+j) \tag{21}$$

Thus, difference waves propagating around the gap are attenuated at a rate of

$$e^{\sqrt{\omega LG/2}} = 19\sqrt{f \cdot 10^{-9}} \quad \text{db per inch} \tag{22}$$

At frequencies even as low as 100 Mhz, the attenuation of difference waves is 6 db per inch. The greater the attenuation, the more independent one location is from its neighbors. Each point on the circumference "knows" only that signal induced locally by the beam, since signals from some distance away are attenuated to insignificance. Therefore, any one voltage monitor point will contain significant position information. (Note, however, that the position sensitivity will be strongly frequency dependent.) Schneider[27] correctly describes a lower cutoff frequency for use of a wall current monitor as a position detector. For our monitor this occurs at 8 Mhz.

The goal of this design, however, is to provide a position insensitive beam current signal. For frequencies high enough to be strongly attenuated by the azimuthal line, the position dependent voltage around the circumference is as described by the static charge model used by Schneider. For lower frequencies, any one point on the circumference effectively "communicates" with other points, reducing the magnitude of any beam position dependence. Both Schneider's static model and calculations done at Fermilab taking the transmission line parameters into account[36] predict that proper summation of signals from four points, at 90° intervals around the gap, will produce a signal with only a few percent position sensitivity for beams within the center half of the device.

Signal summation is performed utilizing DC coupled microstrip combiners on an RT Duroid printed circuit board. Transformer type combiners were rejected because commercial devices typically do not provide the desired few kilohertz to few gigahertz bandwidth. The shunt loaded circuit shown in Figure 16 was chosen because it performs the desired summation with no frequency or source impedance dependence, provided the four input signals are identical. This constraint may seem inappropriate, since the only reason we bother to sum the signals at all is because they are not identical. However, our investigation into the response of transmission line combiners revealed that all possible configurations we considered require some compromise. For example, the typical series loaded combiner, shown in Figure 17, can display dramatic frequency dependence when the source impedance differs from the circuit line impedance, that is, if the combiner lines are not properly back terminated. This is a significant and deciding factor since the source impedance provided by the azimuthal transmission line neither

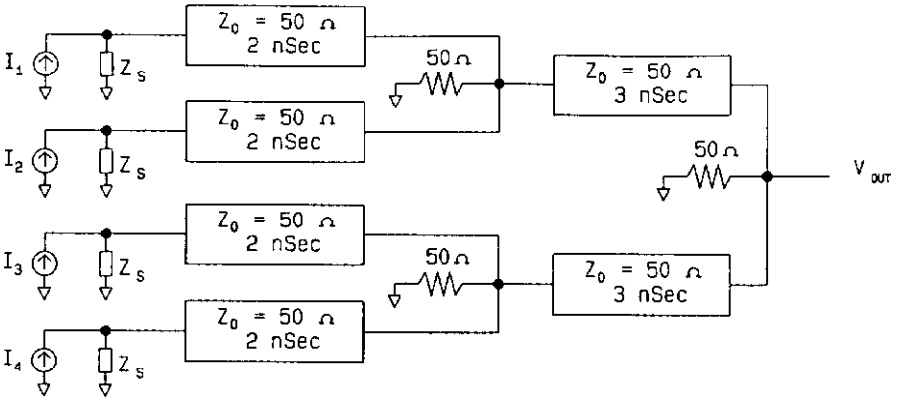

FIGURE 16
SHUNT LOADED COMBINER SCHEMATIC
as used

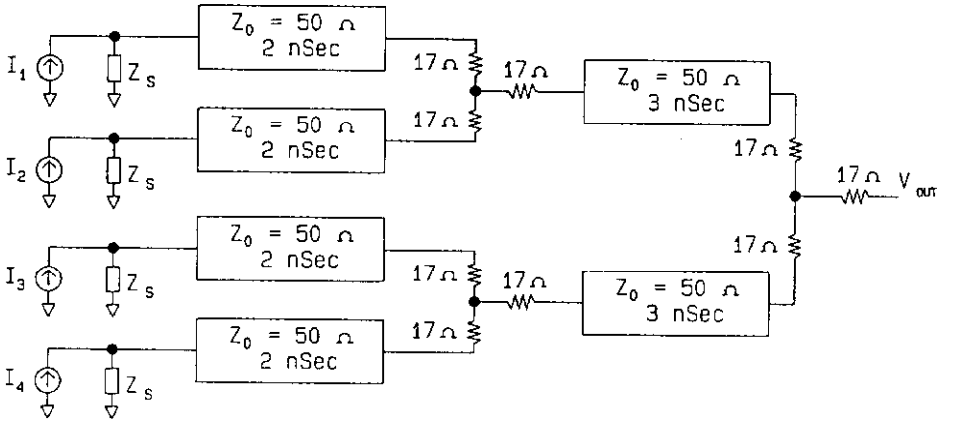

FIGURE 17
SERIES LOADED COMBINER SCHEMATIC
as rejected

matches that of the combiner lines nor remains constant with frequency. This type of combiner, in fact, produces a frequency dependence not only in the difference signal components but also in the sum signal components. Its output will be frequency dependent even when the inputs are identical, that is, when the beam is on center!

The Duroid combiner circuit board is flexible, allowing it to be physically wrapped around one edge of the monitor gap. Good connection is made with the microstrip ground plane there. The four striplines connect to the other side of the gap by small copper straps. Two 120 ohm resistors are omitted from the gap at each 50 ohm tap point to maintain approximately constant resistance per unit arc length around the circumference of the gap. The combined signal is

brought out of the monitor housing on a single 0.141" semi-rigid coax from an SMA connector on the combiner board.

Figures 18 and 19 are photographs of the prototype wall current monitor. Figure 18 shows the clamshell style outer housing, the assorted magnetic toroids, the ceramic gap spanned by many chip resistors, one of the four voltage taps, part of the combiner board, and the output connector. Figure 19 is a close-up of the gap and combiner board.

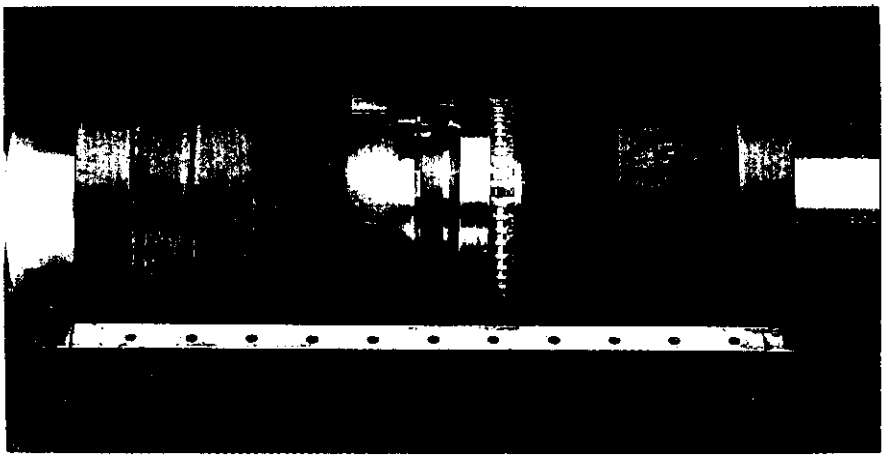

FIGURE 18
WALL CURRENT MONITOR

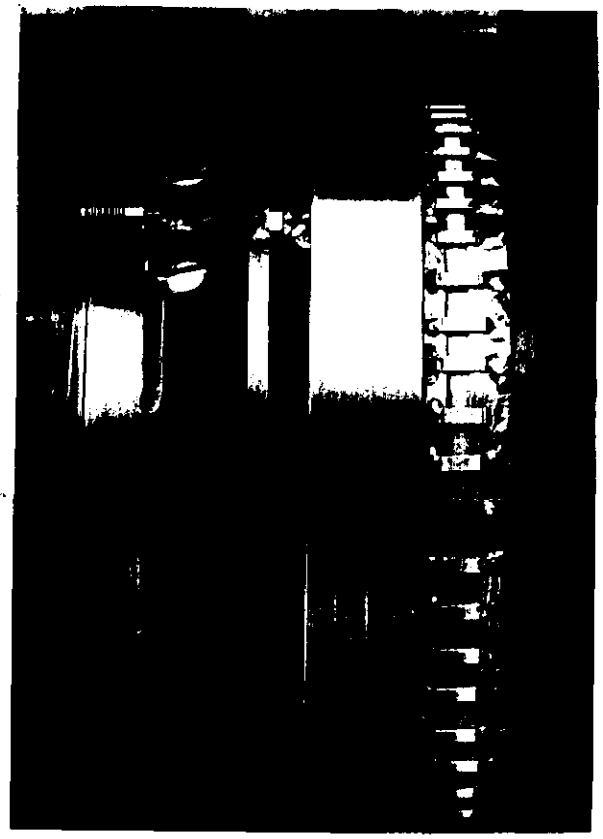

FIGURE 19
WALL CURRENT MONITOR
CLOSE-UP VIEW OF GAP,
RESISTORS, AND
COMBINER BOARD

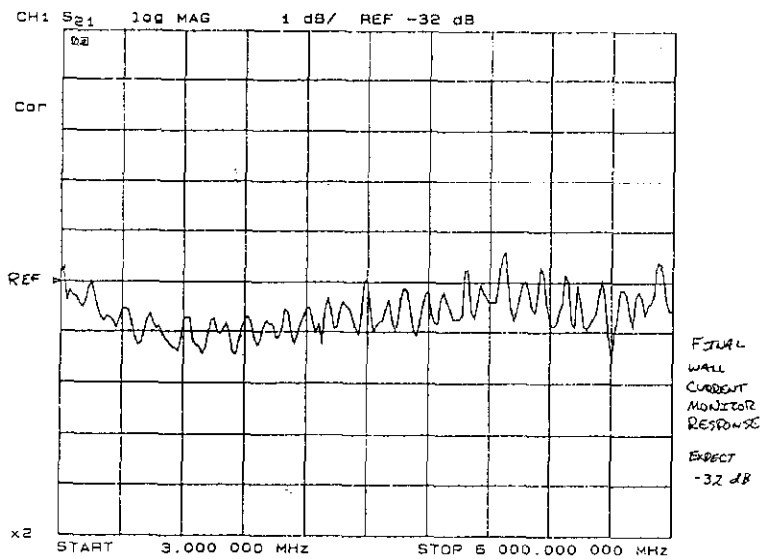

FIGURE 20
WALL CURRENT MONITOR
MEASURED FREQUENCY RESPONSE

A frequency response measurement of the final wall current monitor is shown in Figure 20. The 1db variations, apparent in the measurement at 200 Mhz intervals, are believed to be a remnant of the test fixture and not the wall current monitor itself. Frequency response, flat to within 1db over the full 6 Ghz measurement range of the network analyzer, is demonstrated. The measurement was made with a center conductor placed through the monitor to form a 50 ohm coaxial transmission line system. Tapered cones were used at the ends of the structure to match down to standard coaxial connectors and cables. An identical setup with an outer pipe minus wall current monitor was used as a reference point to which measurements were normalized. Extreme care is necessary in the mechanical design of the test fixture to assure repeatable high frequency electrical measurements each time the fixture is taken apart and reassembled.

One final point to be considered in the application of the extremely wideband wall current monitor is that, by design, it responds to currents in the vacuum chamber wall, whether or not those currents are due to the instantaneous beam current in the monitor. As short beam bunches pass steps, bellows, and other discontinuities in the vacuum chamber wall, they deposit electromagnetic energy in these volumes. The components of that energy with frequencies above the waveguide cutoff frequency of the beam tube are able to then propagate down the pipe. These waves travel at a velocity different from that of the beam and induce currents in the vacuum chamber walls as they go along. The wall current monitor, assuming it has sufficient bandwidth, will faithfully respond to these currents and produce an output signal. Such signals have been directly observed by monitors in the Fermilab Main Ring.[37] These signals, while perhaps valuable for estimating the amount of waveguide energy within the beam tube, are considered as noise when the goal is to measure beam bunch shape.

As a solution to this problem, 12 inch lengths of ceramic cylinders, loaded with broadband microwave absorbing material, are installed in the beam tube immediately upstream and downstream of the wall current monitor. These absorbers provide measured attenuation of the waveguide signals, both on the bench and with beam, of as much as 20db with no effect on the response to true beam currents. Figure 21 shows the spectral output of an earlier monitor

with a single bunch circulating in the Fermilab Main Ring before and after installation of the microwave absorbers. The energy at 1.7 Ghz, above the cutoff frequency for the pipe used on that monitor, is seen to be strongly attenuated. With a single bunch, little true signal energy is present above 100 Mhz. Measurements with other beam distributions confirm that desired signals above 1 Ghz are insignificantly affected.

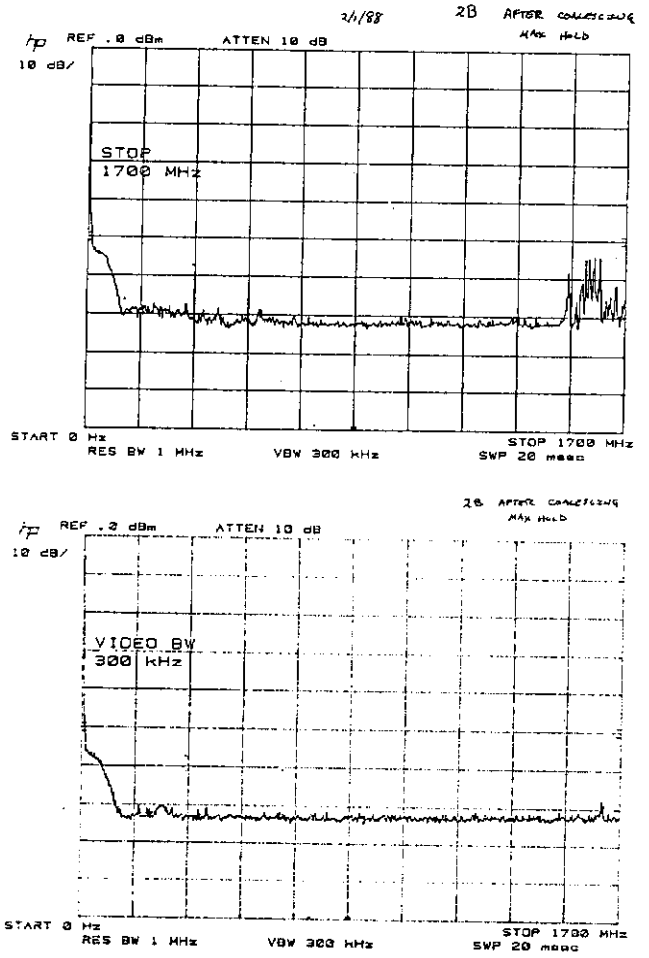

FIGURE 21
MONITOR SPECTRAL OUTPUT FOR SINGLE BEAM BUNCH
BEFORE AND AFTER INSTALLATION OF
UPSTREAM AND DOWNSTREAM MICROWAVE ABSORBERS

This concludes the description of the design parameters and response characteristics of the wall current monitor.

Bibliography

1. F.T. Cole, "Longitudinal Motion in Circular Accelerators", AIP Conf. Proc. No.153 (U.S. Particle Accelerator School), 44-82.

2. D.A. Edwards and M.J. Syphers, "An Introduction to the Physics of Particle Accelerators", AIP Conf. Proc. No.184 (1987-1988 U.S. Particle Accelerator School), 2-189.

3. W.T. Weng, "Fundamentals -- Longitudinal Motion", AIP Conf. Proc. No.184 (1987-1988 U.S. Particle Accelerator School), 243-287.

4. P.S. Martin and S. Ohnuma, "Longitudinal Phase Space in Circular Accelerators", AIP Conf. Proc. No.184 (1987-1988 U.S. Particle Accelerator School), 1941-1968.

5. C. Bovet, et.al., "A Selection of Formulae and Data Useful for the Design of A.G. Synchrotrons", CERN/MPS-SI/Int. DL/70/4, April 1970.

6. J. Gannon, et.al., "Flying Wires at Fermilab", to be published, 1989 Particle Accelerator Conference Proceedings.

7. J. Seeman and J. Sheppard, "Special SLC Developments", 1986 Linear Accelerator Conference Proceedings, September 1986, 214-219.

8. J. Seeman, et.al., "SLC Energy Spectrum Monitor Using Synchrotron Radiation", 1986 Linear Accelerator Conference Proceedings, SLAC-Report-303, September 1986, 441-443.

9. K. Bane, et.al., "Longitudinal Phase Space Measurements in the SLC Linac", to be published, 1989 Particle Accelerator Conference Proceedings.

10. E.J. Soderstrom, et.al., "Fast Energy Spectrum and Transverse Beam Profile Monitoring and Feedback Systems for the SLC Linac", to be published, 1989 Particle Accelerator Conference Proceedings.

11. C.K. Jung, "A High Resolution Synchrotron Light Detector", to be published, 1989 Particle Accelerator Conference Proceedings.

12. J. Nash, "Precision Measurements of the SLC Beam Energy", to be published, 1989 Particle Accelerator Conference Proceedings.

13. K.R. Crandall, "The Delta-T Turn-on Procedure", 1972 Linear Accelerator Conference Proceedings, Los Alamos Laboratory Report LA-5115, 122-125.

14. K.R. Crandall, "The ΔT Tuneup Procedure for the LAMPF 805 Mhz Linac", Los Alamos Laboratory Report LA-6374-MS, June 9176.

15. W.B. Cottingame, et.al., "Noninterceptive Techniques for the Measurement of Longitudinal Parameters for Intense H^- Beams", IEEE Trans. Nucl. Sci., Vol. NS-32, No. 5, October 1985, 1871-1873.

16. W.B. Cottingame, et.al., "Longitudinal Emittance Measurement at the ATS", 1986 Linear Accelerator Conference Proceedings, SLAC-Report-303, September 1986, 101-103.

17. R.L. Witkover, "A Non-Destructive Bunch Length Monitor for a Proton Linear Accelerator", Nucl. Inst. and Methods, Vol.137, No.2, 1976, 203-211.

18. A. V. Feschenko and P.N. Ostroumov, "Bunch Shape Measuring Technique and Its Application for an Ion Linac Tuning", 1986 Linear Accelerator Conference Proceedings, SLAC-Report-303, September 1986, 323-327.

19. G.S. Brown, et.al., "Measurement of Bunch Length with an Image Dissector Tube", IEEE Trans. Nucl. Sci., Vol. NS-30, No. 4, August 1983, 2348-2350.

20. J.C. Sheppard, et.al., "Real time Bunch Length Measurements in the SLC Linac", IEEE Trans. Nucl. Sci., Vol. NS-32, No. 5, October 1985, 2006-2008.

21. R. Chehab, et.al., "Characterization of Low Energy Picosecond Electron Beam Pulses Using Transition Radiation", to be published, 1989 Particle Accelerator Conference Proceedings.

22. J. Borer and R. Jung, "Diagnostics", CERN Accelerator School on Antiprotons for Colliding Beam Facilities, October 1984, CERN/LEP-BI/84-14.

23. G. Lambertson, "Dynamic Devices -- Pickups and Kickers", AIP Conf. Proc. No.153 (1984-1985 U.S. Particle Accelerator School), 1413-1442.

24. T. Linnecar, "The High Frequency Longitudinal and Transverse Pick-ups Used in the SPS", CERN-SPS/ARF/78-17, August 1978.

25. T. Linnecar, "The High Frequency Longitudinal and Transverse Pick-ups in the CERN SPS Accelerator", IEEE Trans. Nucl. Sci., Vol. NS-26, No. 3, June 1979, 3409-3411.

26. R.T. Avery, et.al., "Non-Intercepting Monitor of Beam Current and Position", IEEE Trans. Nucl. Sci., Vol. NS-18, No. 3, June 1971, 920-922.

27. G.C. Schneider, "A 1.5 Ghz Wide-band Beam Position and Intensity Monitor for the Electron-Positron Accumulator (EPA)", 1987 IEEE Particle Accelerator Conference Proceedings, IEEE Catalog No. 87CH2387-9, Vol. 1, 664-666.

28. J. Sodia, et.al., "Timing Jitter Measurements at the SLC Injector", to be published, 1989 Particle Accelerator Conference Proceedings.

29. C. Moore, et.al., "Single-Bunch Intensity Monitoring System Using an Improved Wall Current Monitor", to be published, 1989 Particle Accelerator Conference Proceedings.

30. J. Gareyte, "Beam Observation and the Nature of Instabilities", AIP Conf. Proc. No.184 (1987-1988 U.S. Particle Accelerator School), 343-429.

31. R.H. Siemann, "Bunched Beam Diagnostics", AIP Conf. Proc. No.184 (1987-1988 U.S. Particle Accelerator School), 430-471.

32. R. Littauer, "Beam Instrumentation", AIP Conf. Proc. No.105 (1982 U.S. Particle Accelerator School), 869-953.

33. V.K. Bharadwaj, "Beam Transfer from the Core of the Accumulator to the Main Ring in the Fermilab Source", 1987 IEEE Particle Accelerator Conference Proceedings, IEEE Catalog No. 87CH2387-9, Vol. 2, 1022-1024.

34. J. Marriner, "Review of the Physics, Technology and Practice of Stochastic Beam Cooling", 1987 IEEE Particle Accelerator Conference Proceedings, IEEE Catalog No. 87CH2387-9, Vol. 3, 1383-1387.

35. T. Ieiri and G. Jackson, "A Main Ring Bunch Length Monitor by Detecting Two Frequency Components of the Beam", Fermilab TM-1600, June 1989.

36. J. Crisp, Fermilab, unpublished.

37. J.E. Griffin and J.A. MacLachlan, "Direct Observation of Microwaves Excited in the Fermilab Beam Pipe by Very Narrow Bunches", IEEE Trans. Nucl. Sci., Vol. NS-32, No. 5, October 1985, 2359-2361.